Heartbeat rate measurement using microwave systems: single-antenna, two-antennas, and modeling a moving person

Sarah El-Samad, Dany Obeid, Gheorghe I. Zaharia, Sawsan Sadek, Ghaïs El Zein

Heartbeat rate measurement using microwave systems: single-antenna, two-antennas, and modeling a moving person

Sarah El-Samad[1,2], Dany Obeid[1], Gheorghe Zaharia[2], Sawsan Sadek[1], Ghais El Zein[2]

Abstract: This paper presents a microwave system for heartbeat rate measurement. This system is based on using a vector network analyzer and horn antennas. The system generates a continuous wave signal toward a person's chest then the reflected signal is analyzed. The phase difference between the emitted and the reflected signals contains information about the chest movement; hence, the heartbeat rate can be extracted. In this work, several scenarios for detecting the heart activity are considered. The first scenario aims to provide a comparative study for using single-antenna and two-antennas microwave systems. Several radiated powers are considered in this scenario. Simultaneously with the microwave system, a wireless electrocardiograph is used as reference in order to determine the accuracy of the system. Measurements are performed in both cases when breathing normally and when holding the breath. The second scenario aims to test the ability of detecting the heartbeat activity of a person while moving. Measurements are performed while the subject walks towards the radar. Modeling is used for this purpose. The operating frequency used is 20 GHz in both scenarios. Signals are processed using wavelet transform and results show the ability to extract the heartbeat rate even with the presence of body movement.

Sarah Samad
sarah.samad@insa-rennes.fr

Dany Obeid
dany.obeid@gmail.com

Gheorghe Zaharia
gheorghe.zaharia@insa-rennes.fr

Sawsan Sadek
sawsan.sadek70@gmail.com

Ghais El Zein
ghais.el-zein@insa-rennes.fr

1. Doctoral School of Science and Technology, Lebanese University, Lebanon
2. Univ Rennes, INSA Rennes, CNRS, IETR (Institut d'Electronique et de Telecommunications de Rennes) UMR 6164, F 35000 Rennes, France

Keywords: single-antenna microwave system; two-antennas microwave system; moving person; electrocardiograph; heartbeat rate; signal processing; wavelet decomposition

1 Introduction

Nowadays, contactless monitoring of vital signs is needed in medical surveillance applications and in healthcare, especially for infants at risk, sudden infant syndrome or burn victims where the use of the traditional electrodes to measure cardiopulmonary signals is not possible. Due to the microwave sensitivity toward tiny movements, radar has been employed as a noninvasive monitoring system of human cardiopulmonary activity [1]. Several radar technologies are presented in the literature for the vital signs extraction: the ultra-wideband (UWB) radars, the frequency modulated continuous wave (FMCW) radars, and the continuous wave (CW) Doppler radars. Each of these types has its own advantages and disadvantages. The advantage of the UWB radar is its ability to detect the patient – system distance and the breathing rate for one or more persons [2]. On the other side, UWB is not feasible in terms of system integration and low-power operation, especially for short range applications [3]. In contrast, CW and FMCW systems allow higher level of system integration and lower power operation. Note that the CW radar is not able to extract range resolution like UWB and FMCW radars [4]. Although FMCW radar allows measuring the distance of the target [5], the CW radar is superior to FMCW due to its higher measurement accuracy, less complex hardware architecture, and simpler signal processing techniques [6]. Therefore, for applications that only require displacement information regardless of the target range, CW radar is a better option for non-contact vital sign detection [7]. Therefore, the CW it is utilized in this work. According to Doppler effect, a constant frequency signal reflected off an object having a varying displacement has a time-varying phase [1] which contains the heartbeat and respiration information. Note that the average peak-to-peak chest motion caused by the respiration is between 4 and 12 mm, and caused by the heartbeat alone is between 0.2 and 0.5 mm [8]. At rest, the respiration frequency of an adult varies between 0.2 and 0.34 Hz which means a respiration rate between 12 and 20 Breathes per minute (Bpm) [9]. Moreover, the heartbeat frequency of an adult changes within 1 and 2 Hz, which means a heartbeat rate between 60 and 120 beats per minute (bpm) [8].

In this work, two scenarios are considered: First, in order to test the accuracy of the single-antenna system compared to the two-antenna system, a comparative study is realized for a person while holding the breath. In fact, using a single antenna will reduce the number of components of the final measurement system; hence it will reduce the cost. After that, the person breathes normally and the heartbeat rate is extracted using single-antenna microwave system. The accuracy of the obtained results demonstrates the possibility of extracting the heartbeat signal using a single-antenna microwave system for a person while breathing normally.

The second scenario is considered by testing the ability of detecting heartbeat rate of a moving patient inside a room. The person is walking toward the radar. This scenario is based on modeling and wavelet-based techniques are applied for heartbeat rate extraction in both cases.

The rest of this paper is organized as follows: Section 2 presents the measurement setup of the two systems and the obtained results for a person holding the breath. Section 3 presents results of a single antenna VNA system for a person breathing normally. Section 4 presents the modeling of the received signal for a moving forward person and the processing technique and the obtained results. Section 5 concludes the work.

2 Comparison between Heartbeat Rates extracted from single and two-antenna microwave systems for a non-breathing person

Previous works [10] used the two-antenna microwave system to demonstrate the possibility of detecting the heartbeat activity. The first and the second antennas were used for the emission and the reception respectively. This system was used to measure the time-varying phase of the S_{21} parameter for different operating frequencies and different radiated powers. In addition, a study using a 16 GHz single-antenna VNA system was realized to measure the S_{11} phase variation for a person while holding the breath [11]. In this case, the same antenna is used for both emission and reception. In this section, a comparison between Heartbeat Rates extracted from single and two-antenna microwave systems for a non-breathing person is done to test the accuracy of the heartbeat rate of the single-antenna system relatively to the two-antenna system.

2.1 Measurement setup

The two systems are based on a VNA and one or two horn antennas. These components make the installation fast and simple. The used VNA is HP N5230A 4 ports PNA-L. The VNA is one of the main basic systems used for microwave measurements and RF applications. In addition, the VNA allows tuning both frequency and power. It allows the control of different parameters like sweep time and the number of sampling points. Furthermore, it measures the phase and amplitude of S parameters. In particular, a VNA measures the time variation of the phase of the parameters S_{21} or S_{11} which are used in this study. In the case of two-antenna systems, S_{21} phase variation is measured. When using a single-antenna microwave system, S_{11} phase variation is measured. The antennas used are LB-42-25-C2-SF with operating frequencies between 18 and 26.5 GHz. The operating frequency is chosen to be f_o = 20 GHz due to two reasons: the first reason is to obtain higher phase variation as it is directly proportional to the frequency. The second reason is due to the equipment's limitation (2 – 20 GHz of the VNA). Note that the antenna gain depends on the frequency. Table 1 shows the antenna gain for different operating frequencies [10].

Table 1 Antenna gain

Frequency (GHz)	Gain (dBi)
18	23.6
19	23.9
20	24
21	24.5
22	24.9
23	24.8
24	24.9
25	25.4
26	25.4

According to this table, the antenna gain at 20 GHz is 24 dB. The IF bandwidth is chosen to be 500 Hz resulting from a compromise between the signal noise reduction and the sweep time. As the sweep time was 23 secs, the number of samples was set at 12801 by the VNA; hence the sampling frequency is 557 Hz. The 23 seconds is selected to avoid too long stopping breathing when the person is the breath. The measurements were performed for a healthy 54-years old person. The distance between the antennas and the person is 1 meter. Considering the antenna gain (24 dB), the cables losses (2 dB) and the emitted power at the VNA output (-24, -29, -34 and -39 dBm), the radiated power P_r is -2, -7, -12 and -17 dBm, respectively. Measurements with several values of the emitted power allow determining the minimum power required to accurately extract the heartbeat rate while limiting the risks of exposure to the electromagnetic waves for the patient and the medical staff. The highest radiated power (- 2 dBm), this corresponds to a surface reception power density of about 5 nW /cm^2, which is very low compared to the FCC exposure

level limit (580 μW /cm^2). In addition, the FCC allows a Specific Absorption Rate (SAR) limit of 1.6 W/kg, as averaged over one gram of tissue, hence the measurements performed are considered as safe.

Note that an ECG is used simultaneously with the system as a reference system. Table 2 presents the measurement setup characteristics for this experiment and Fig. 1 presents the measurement system with single antenna vs. electrocardiograph.

Table 2 Measurement setup

System specifications	
Operating frequency f_o (GHz)	20
Radiated power P_r (dBm)	-2, -7, -12, -17
Number of points	12801
Time window (sec)	23
Sampling frequency (Hz)	557
Antennas number	1 or 2
Subject Information	
Gender/ Age (y)	M/54
Position/ Side	Setting/ Front
Distance (m)	1
Breathing	No
Position	Setting/ Front

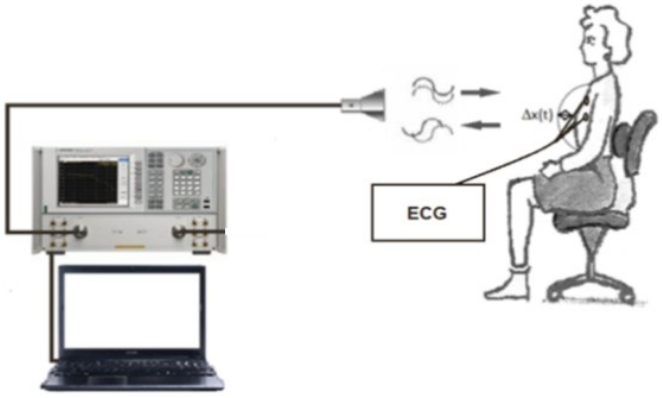

Fig. 1 Measurement system with single antenna vs. electrocardiograph

2.2 Signal processing and obtained results

In this section, measurements were performed for a person holding the breath for both single-antenna and two-antennas microwave systems. Figs. 2 and 3 present the phase variation (PV) of S_{11} and S_{21} respectively, at radiated powers: -2, -7, -12 and -17 dBm.

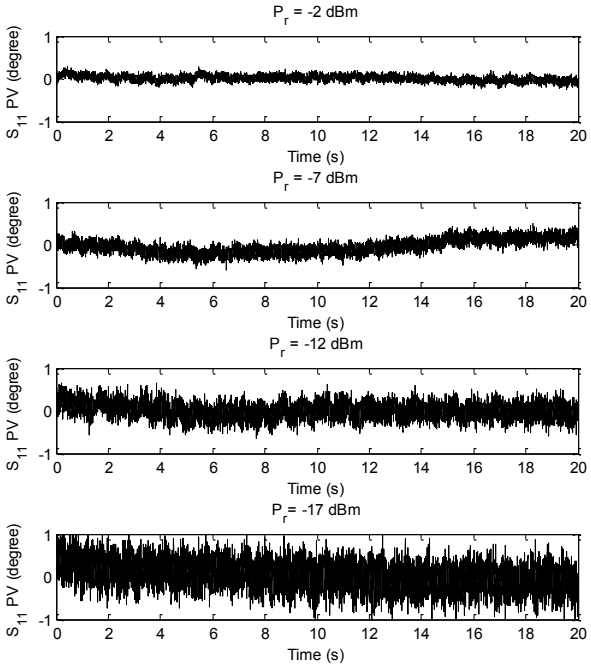

Fig. 2 Phase variation of S_{11} for a person holding his breath for different radiated powers using the single-antenna microwave system.

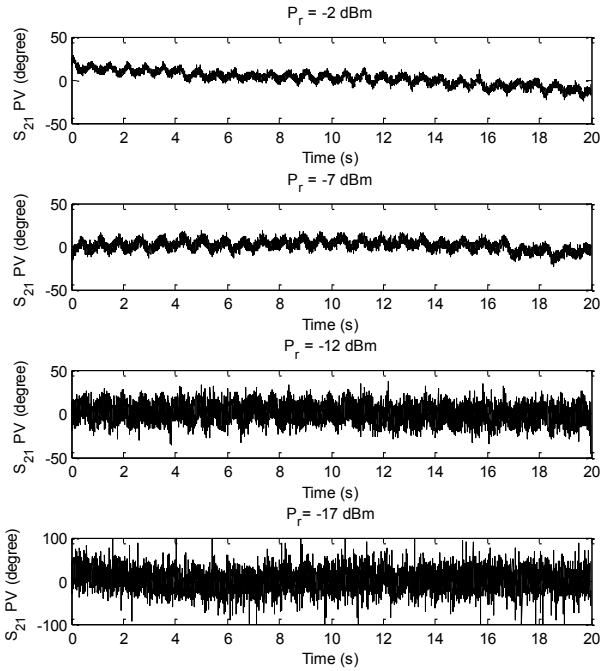

Fig. 3 Phase variation of S_{21} for a person holding his breath for different radiated powers using the two-antenna microwave system.

It is observed that the phase variation of S_{21} is clearer and larger than the phase variation of S_{11}; hence, the heartbeat signals are clearer in the case of S_{21} phase variation. In both cases, the SNR decreases with the decrease of the radiated power; thus, a smoothing method is required in order to reduce

noise and extract the heartbeat signal, especially for lower radiated powers. This method is based on a sliding window. It replaces a given point by the average of its surrounding points. I.e. consider a signal X with N samples, $X = [X(0), ..., X(N\text{-}1)]$, the sample $X_S(i)$ of the smoothed signal is computed with the following relation:

$$X_S(i) = \frac{1}{n}\sum_{k=i-m}^{i+m} X(k) \quad (1)$$

where n = 2m+1 is the length of the smoothing window. Note that i should be between m and N-m-1. Otherwise, the length of the smoothing window is decreased. When n increases, the variation of the heartbeat signal may reduce. On the other hand, when n decreases, the heartbeat signal could not be detected correctly due to the presence of noise; hence, a compromise should be done in order to reduce the noise without losing the significant peaks of the recorded phase. n = 199 was chosen after several trials. After noise reducing using smoothing technique, peak detection is applied, and then heartbeat rate is extracted. Fig. 4 presents the peak detection of the phase variation of S_{11} when using the single-antenna microwave system and Fig. 5 presents the peak detection of the phase variation of S_{21} when using the two-antennas microwave system, after applying smoothing with n = 199 and for different radiated powers: -2, -7, -12 and -17 dBm. Both figures contain the ECG signal measured simultaneously with the VNA signal.

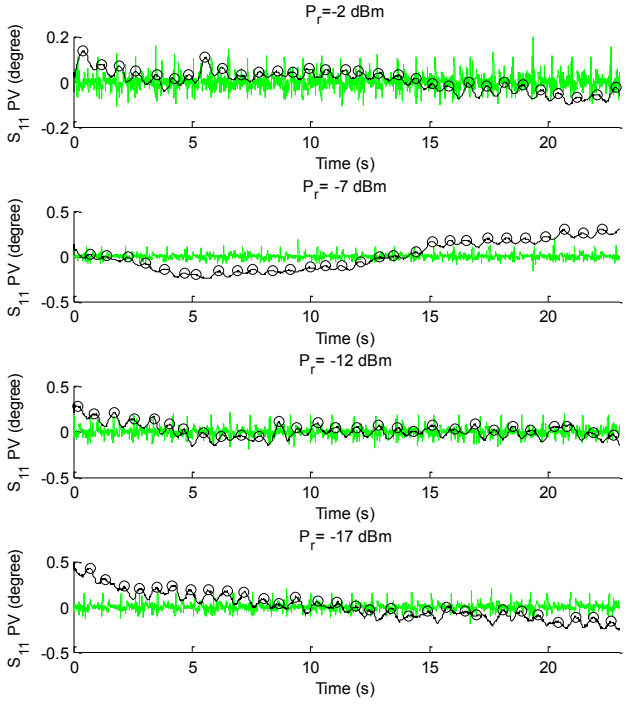

Fig. 4 Peak detection for the phase variation of S_{11} after applying smoothing with n = 199 at P_r = -2, -7, -12 and -17 dBm and f_e = 20 GHz (Black), ECG signal (Green).

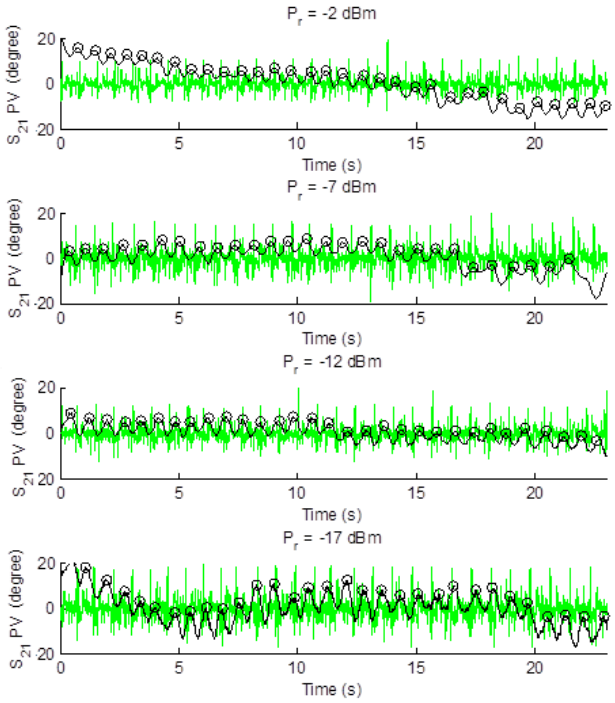

Fig. 5 Peak detection for the phase variation of S_{21} after applying smoothing with n = 199 at P_r = -2, -7, -12 and -17 dBm and f_e = 20 GHz (Black), ECG signal (Green).

After peak detection of the heartbeat signal, the heartbeat rate expressed in beats per minute (bpm) is calculated using the following relation:

$$HR = \frac{60(N-1)}{d_1 + d_2 + \cdots + d_{N-1}} \quad (2)$$

where N is the peaks number and d_k is the duration of the interval determined by 2 successive peaks expressed in seconds. The relative error between HR of the microwave system and HR of the ECG is calculated using the following relation

$$RelativeError = 100 \times \frac{HR_{VNA} - HR_{ECG}}{HR_{ECG}} \quad (3)$$

Table 3 presents the heartbeat rate extracted from the single-antenna microwave system ($HR_{VNA\text{-}SA}$), the heartbeat rate extracted from the ECG (HR_{ECG}) and the relative error between $HR_{VNA\text{-}SA}$ and HR_{ECG}. Table 4 presents the heartbeat rate extracted from the two-antenna microwave system ($HR_{VNA\text{-}TA}$), the heartbeat rate extracted from the ECG (HR_{ECG}) and the relative error between $HR_{VNA\text{-}TA}$ and HR_{ECG}.

Table 3 Comparison between $HR_{VNA\text{-}SA}$ and HR_{ECG} using the single-antenna microwave system

Radiated power (dBm)	$HR_{VNA\text{-}SA}$ (bpm)	HR_{ECG} (bpm)	Relative Error (%)
-2	80	75	7
-7	78	72	8
-12	74	69	7
-17	79	73	8

Table 4 Comparison between $HR_{VNA\text{-}TA}$ and HR_{ECG} using the two-antenna microwave system

Radiated power (dBm)	$HR_{VNA\text{-}TA}$ (bpm)	HR_{ECG} (bpm)	Relative Error (%)
-2	84	78	8
-7	77	72	7
-12	81	76	7
-17	80	75	7

According to the American National Standard [12], medical devices measuring the heartbeat rate should have a relative error lower than 10% or 5 bpm; hence, the obtained results are acceptable for both systems with maximum relative error of 8%.

After holding breath, the next step is performing measurements using single-antenna microwave system for a breathing person to show the possibility of extracting heartbeat rate in this case.

3 Results for normally breathing person using single-antenna microwave system

3.1 Measurement setup

In this section, we describe the measurement results obtained when the same person is breathing normally. The measurements are performed while using the single-antenna system. These measurements are performed to confirm that the single-antenna system is able to extract the heartbeat rate for a breathing person. The person was sitting at 1 m from the system with always the ECG system used as reference. Fig. 6 presents the phase variation of S_{11} for a breathing person at different radiated powers: -2, -7, -12 and -17 dBm.

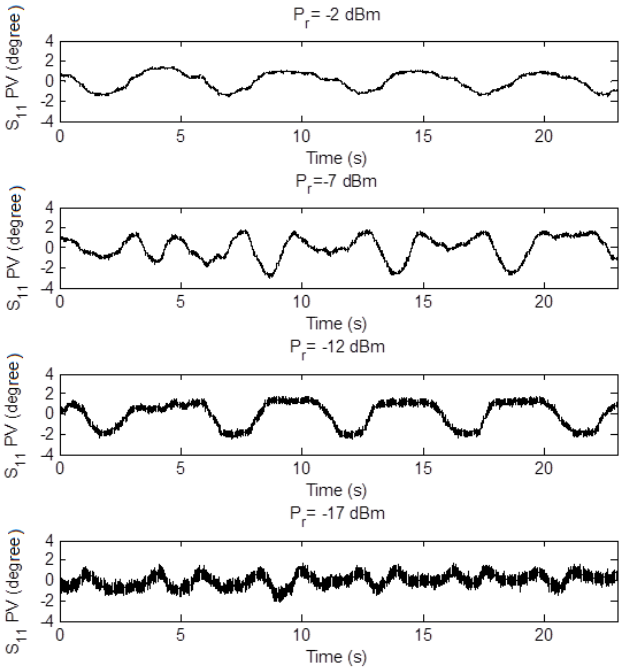

Fig. 6 Phase variation of S_{11} for a breathing person for different radiated powers.

As shown, the SNR decreases with the decrease of the radiated power. In addition, the phase variation of S_{11} is mainly due to the respiration; hence, signal processing is required to reduce the influence of the respiration and the noise in order to extract the heartbeat signal.

3.2 Signal processing using wavelet decomposition

As chest motion due to respiration is much bigger compared to that due to the heartbeat, an advanced signal processing technique is required in order to reduce the respiratory signal and then extract the heartbeat signal. In [13] it was shown that classical filters are able to extract successfully the heartbeat signal, but due to the distortion of the filtered signal during the transitive regime, the relative error of heartbeat can be increased. In addition, Fast Fourier transform (FFT) converts a signal from time domain to frequency domain rapidly. Then, the frequency having the maximum amplitude between 1 and 2 Hz is chosen. FFT gives accurate results but an extra error may occur because real frequency may not match the FFT frequency points, the power spectrum is spreading at the adjacent frequencies. In addition, the variation of the HR over the time could not be tracked. To solve this problem, Short-Time Fourier Transform is proposed (STFT). This technique is based on applying the Fourier transform over portions of the signal, namely windows. This allows analyzing the signal in both time and frequency domains. Short time window results in high resolution in time and poor resolution in frequency, while large window results in poor resolution in time, but high resolution in frequency. The problem of the STFT is solved by using the wavelet transform [14]. The processing technique used in this study is the wavelet decomposition. The wavelet technique consists of splitting the signal into several signals; each of these signals corresponds to a frequency band. There are two types of wavelets: continuous wavelets transform (CWT) and discrete wavelets transform (DWT). DWT is a fast and non-redundant transform. The DWT is used in order to extract the heartbeat signal from the cardiopulmonary signal. The DWT ($W_{j,k}$) of a signal $f(t)$ is given by the scalar product of $f(t)$ with the scaling function (i.e. the wavelet basis function) $\emptyset(t)$ which is scaled and shifted:

$$W_{j,k} = f(t), \emptyset_{j,k}(t) \geq \int_{-\infty}^{+\infty} f(t)\, \emptyset_{j,k}(t) dt \tag{4}$$

The basis function is given by:

$$\emptyset_{j,k}(t) = 2^{-j/2} \emptyset(2^{-j} t - k T_S) \tag{5}$$

where j is the j^{th} decomposition level or step and k is the k^{th} wavelet coefficient at the j^{th} level [11]. The variables j and k are integers that scale and dilate $\emptyset$ to generate wavelets. Several families exist in the wavelet decomposition like Daubechies, Coiflets, Symlets, etc. The difference between wavelet families makes compromise between how compactly they are localized in time and how smooth they are. Within each wavelet family, the number of coefficients and the iterations used in the wavelets are classified as subclasses [15]. The suitable wavelet family is chosen depending on data. The DWT applies a successive low-pass and high-pass filtering of the discrete time-domain signal and decomposes the signal into decomposition '*D*' and approximation '*A*'. '*A*' represents the low-pass filtered signal and '*D*' represents the high-pass filtered signal [15]. The decomposition is repeated and the frequency resolution is increased. In general, if *n* is the decomposition level, A_n contains frequencies between 0 and $f_s/2^{n+1} \wedge D_n$ contains frequencies between $f_s/2^{n+1}$ and $f_s/2^n$, where f_s is the sampling frequency. The DWT principle is resumed in Fig. 7.

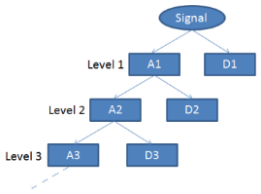

Fig.7 Wavelet decomposition.

The original signal can be reconstructed using the following relation:

$$S_{reconstructed} = A_N + D_N + D_{N-1} + \cdots + D_1 \tag{6}$$

where N is the maximal value of the decomposition level. The wavelet family chosen should fulfill the properties of the signal. The reconstructed signal has to be as close as possible to the original signal with fewer decomposition levels [16]. The suitable wavelet should have the best reconstruction of the original signal compared to other families; hence, the error between the original signal and the reconstructed signal should be the smallest. The indicator of the error between the original signal $x(n)$ and the reconstructed signal $\hat{x}(n)$ is the Root Mean Square Error (*RMSE*):

$$RMSE = \sqrt{\frac{\sum_{n=0}^{L-1} |x(n) - \hat{x}(n)|^2}{L}} \tag{7}$$

where L is the samples number of the signal x.The *RMSE* is calculated for all available signals for different wavelet types; then the mean of the *RMSE* of all available signals is calculated for each wavelet type according to the following relation:

$$RMSEmean_{wavelettype} = \frac{\sum_{p=1}^{4} RMSEofthesignal(p)(wavelettype)}{4} \tag{8}$$

where p is the power index (p = 1, 2, 3 and 4 for signals extracted at radiated powers -2, -7, -12 and -17 respectively). Bior 2.4 is chosen after the mean *RMSE* calculation for all wavelet types. Bior 2.4 has the lowest mean *RMSE* compared to the others. The heartbeat rate for an adult is between 60 and 120 beats per minute, hence the frequency of the heartbeat is located between 1 and 2 Hz. A re-sampling method is necessary in order to obtain the decomposition of the signal in the appropriate frequency band. Thus, a conversion of the sampling frequency from 666.7 Hz to 512 Hz is applied in order to obtain a band of frequencies between 0 and 1 Hz at the 8th approximation. Two processes are performed for the re-sampling implementation: firstly, a linear interpolation of the given discrete signal to a continuous signal is applied; then applying sampling to the interpolated signal at the new coordinate points [17]. Eliminating the 8th approximation from the reconstructed signal gives a signal with the frequency band is between 1 to 256 Hz. As mentioned, the respiratory amplitude is higher than the heartbeat amplitude; hence, the role of processing techniques is to significantly reduce the respiratory signal from the cardio-respiratory signal. In general, respiratory frequency is between 0.2 and 0.34 Hz. Hence, the signal A_8 that contains this frequency band is excluded from $S_{reconstructed}$. S_{D18} is given by: $S_{D18} = S_{reconstructed} - A_8 = D_8 + D_7 + D_6 + D_5 + D_4 + D_3 + D_2 + D_1$. It is named S_{D18} because it contains all decompositions with levels between 1 and 8. As the heartbeat frequency is between 1 and 2 Hz, it belongs to S_{D18}. After extracting S_{D18}, smoothing method with n = 199 is applied to reduce the noise. Then peak detection is used in order to calculate the heartbeat rate. Fig. 8 presents the smoothed S_{D18} signal at different radiated powers.

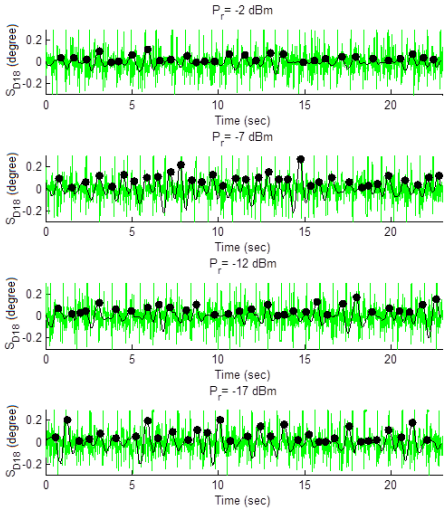

Fig. 8 Peak detection applied to the smoothed S_{D18} at P_r = -2, -7, -12 and -17 dBm and f_o = 20 GHz (Black), ECG signal (Green).

3.3 S_{D18} pass band reducing

In this work, A_8 is eliminated from $S_{reconstructed}$ to reduce the respiratory signal and keep the heartbeat signal which is above 1 Hz; hence all the decompositions from 1 to 8 are kept. Then smoothing, peak detection, and heartbeat rate extraction are applied. Note that the heartbeat signal is not situated in the entire S_{D18} frequency band which is between 1 and 256 Hz. In this part, several decompositions are eliminated to reduce the bandwidth of the signal and keep the effective signal; hence D_8, $D_8 + D_7$, $D_8 + D_7 + D_6$, …, $D_8 + D_7 + D_6 + D_5 + D_4 + D_3 + D_2 + D_1$ are extracted and smoothed in order to reduce the noise. The relative errors between HR_{ECG} and $HR_{VNA\text{-}SA}$ obtained from these signals are calculated. Table 5 presents the relative error between the single-antenna-microwave system and the ECG using wavelet decomposition for different S_{Dn8}. S_{Dn8} is a summation between the decomposition n till the decomposition 8.

Table 5 Relative errors between the single-antenna microwave system at different S_{Dn8} and the ECG

S_{D88}	S_{D78}	S_{D68}	...	S_{D18}
6.2	2.5	1		1
17	17	17		17
4	3	3		3
4	4	4		4

As result, $D_8 + D_7$ gives better results than D_8, $D_8 + D_7 + D_6$ gives better results than $D_8 + D_7$. Finally, from $D_8 + D_7 + D_6$, the relative errors are the same. As conclusion, the band between 1 and 8 Hz is sufficient to extract the heartbeat rate successfully without adding frequencies above 8 Hz. Also, a band slightly wider than [1 Hz, 2 Hz] must be used to have a small error. In other words, the details in the higher bands help to better describe the heartbeat signal which is not a pure sinusoidal.

3.4 Obtained results

Table 6 presents the heartbeat rate extracted from the single-antenna microwave system ($HR_{VNA\text{-}SA}$), the heartbeat rate extracted from the ECG signal (HR_{ECG}) and finally the relative errors between $HR_{VNA\text{-}SA}$ and HR_{ECG} for a breathing person and with different radiated powers.

Table 6 $HR_{VNA\text{-}SA}$ and HR_{ECG} For a breathing person with different radiated powers

Radiated power (dBm)	HR_{VNA-SA} (bpm)	HR_{ECG} (bpm)	Relative Error (%)
-2	81	80	1
-7	90	77	17
-12	82	80	3
-17	86	83	4

Even at low power, heartbeat rates can be extracted and the relative errors are less than 4%; hence, the obtained results are acceptable. However, at -7 dBm, the relative error is 17%, hence new measurements should be conducted to confirm the results and lead to a good interpretation.

4 Models and processing of a moving person

Previous researches have been focused on the non-contact detection of the heartbeat rate of fixed subjects using wireless systems under different conditions. However, the subject can move with a Random Body Movement (RBM). RBM is considered as a significant source of noise and the most challenging issue for the accurate measurement of the heartbeat rate using touch less radar systems. RBM is mostly bigger than the chest movements due to tiny vital signs that have several millimeters to centimeters; hence the RBM signal is able to hide the signal of interest. Some studies resolved the problem of RBM by using multiple transceivers detecting from different sides of the human body [18]. In general, when the person moves between two radars, from one to the other, the body moves toward one of them and away from the other radar. When combining the two signals, the body motion can be canceled. Other methods studied the RBM elimination using either two-frequency radar [19] or multi-frequency interferometric radar [20]. However, these studies have some drawbacks. Firstly, the use of multiple radar systems to cancel RBM increases the system complexity. Secondly, the alignment of different systems could be a potential bottleneck for accurate detection. In this section, models of chest motion with the presence of 1-D body motion are performed. A case of an old person that performs a uniform movement in his room is taken into consideration. One radar system is used to emit and then detect the vital signs. After that, wavelet method is used to extract the heartbeat signal. Fig. 9 presents the measurement setup for a moving person with an operating frequency of 20 GHz and emitted power of -19 dBm. This emitted power corresponds to a radiated power of 3 dBm.

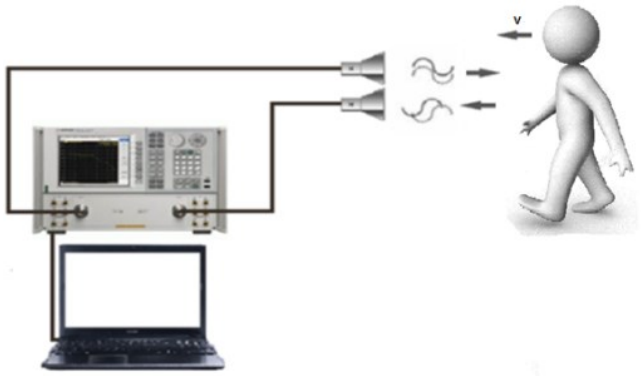

Fig. 9 Detection setup for a moving person (v is the person's velocity)

4.1 Modeling of a chest motion when moving forward

In this scenario, the person moves towards the system and $\Delta x(t)$ is the variation of the person-system distance determined by the movement of the person and his chest motion due to heartbeat and respiration. Therefore, $\Delta x(t)$ can be computed as [21]:

$$\Delta x(t) = -vt + x_h(t) + x_r(t) + n(t) \quad (9)$$

where v is the velocity of the person. Note that the '-' sign is due to the movement forward (*i.e.*, to the measurement system), $x_h(t)$ is the heartbeat motion, $x_r(t)$ is the respiratory motion and $n(t)$ is the additive noise. Based on experiments, the additive noise is a Gaussian noise.

The person starts moving at a distance of 3 m from the antennas and walks to the system with a constant velocity v = 0.25 m/s; hence the relation of the walking forward is $-vt$. The person stopped at a distance of 1 m from the system; hence the person is walking during 8 s. The operating frequency chosen for this work is 20 GHz and the phase at t = 0 s has an arbitrary value which is chosen to be 0°. In fact, the maximum variation of the phase ranges between -180° and

+180°, hence each time the phase reaches the -180°, it will permute to +180° and vice versa.

The heartbeat signal can be expressed by $x_h = A_h sin(2\pi f_h t + \emptyset_{oh})$, where A_h is the amplitude of chest movement due to heartbeat, f_h is the heartbeat frequency and $\emptyset_{oh}$ is the heartbeat sine wave phase at t = 0 and chosen to be 90°. The heartbeat rate considered for this signal is 70.73 beats/min. The displacement of the chest due to heartbeat is 0.5 mm.

The respiration is also modeled as a sine wave; hence $x_r = A_r sin(2\pi f_r t + \emptyset_o)$, where A_r is the amplitude of the chest movement due to respiration, f_r is the respiratory frequency and $\emptyset_o$ is the phase at t = 0 s is an arbitrary value and chosen to be 90°. The displacement of the chest due to respiration is A_r = 12 mm and the respiration frequency is f_r = 0.25 Hz.

4.2 Phase noise model

Eliminating the noise affecting the signal quality is considered as one of the biggest challenges. Relations (10) and (11) present the signal power at the input of VNA system and the signal to noise ratio (SNR) of VNA input respectively:

$$P_S(dBm) = P_e(dBm) + G_e(dB) + G_r(dB) - A_1(dB) - Refl(dB) - A_2(dB) \quad (10)$$

$$\begin{aligned} SNR_{VNAinput}(dB) &= P_S(dBm) - P_n(dBm) \\ &= P_e(dBm) + G_e(dB) + G_r(dB) \\ &\quad - A_1(dB) - Refl(dB) - A_2(dB) \\ &\quad - P_n(dBm) \end{aligned} \quad (11)$$

where P_e is the emitted power, G_e is the antenna gain at the emission, G_r is the antenna gain at the reception, $A_1(dB) + A_2(dB)$ are the round trip free space losses, $Refl$ is the reflection loss on the human body and P_n is the noise power at the VNA input.

Note that global free space losses have the following relation:

$$\begin{aligned} A(dB) = A_1(dB) + A_2(dB) &= 2A_1(dB) \\ &= 40log_{10}(4\pi d/\lambda) \end{aligned} \quad (12)$$

Because this study presents the case of a person moving toward the VNA system, the distance '*d*' between the person and the VNA system decreases; hence, based on (11), the *SNR* of the input signal increases when the person is getting closer to the Doppler radar. *SNR* of the phase variation is certainly related to the signal *SNR*; but no direct relation between *SNR* of the signal and *SNR* of the phase is presented, nor between phase noise and distance between the person and the radar. Measurements are used to find a relation between the signal noise and the distance. As seen in (10), for each emitted power P_e of a fixed person (distance is fixed), the signal power at the VNA input is fixed. In addition, for each emitted power used for the fixed person, the variance of the phase noise is assumed to be constant. From S_{21} phase measurements, the variance of the phase noise is extracted for several values of the emitted power. Then, a relation between the emitted power and the variance of the phase noise is found from these measurements. Hence, a relation between the signal power at the VNA input and the phase noise variance is found from the relation extracted from measurements and (10). Fig. 10 presents the S_{21} phase extracted at different emitted powers: -19, -24, -29, -34, -39 and -44 dBm for a person holding his breath. These values correspond respectively to radiated powers: 3, -2, -7, -12, -17 and -22 dBm. The sampling frequency is 20 kHz. The person is fixed at a distance of 1 m from the antennas system. The gain of each antenna at 20 GHz is 24 dB.

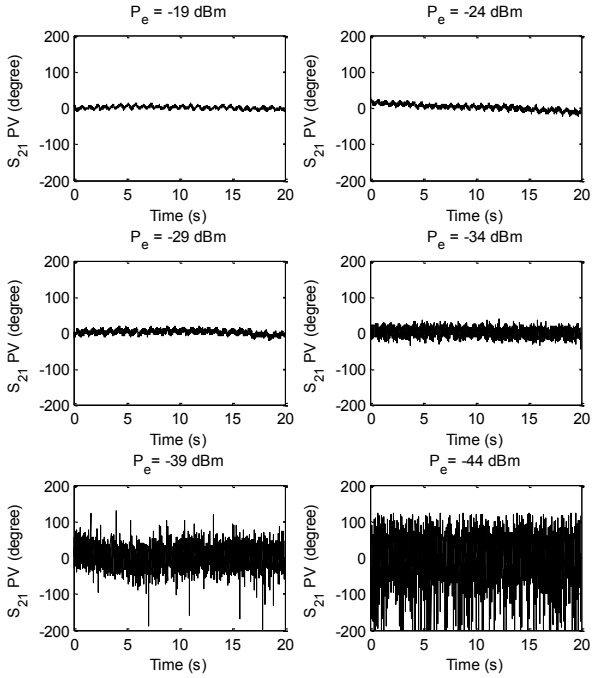

Fig. 10 Phase variation of S_{21} at P_e = -19, -24, -29, -34, -39 and -44 dBm and f_e = 20 GHz

The variation of the S_{21} phase contains the heartbeat signal and the additive noise; hence, the heartbeat signal should be eliminated to extract the variance of the phase noise. The heartbeat signal is extracted by using a sliding uniform

smoothing window with the length $n = 199$. When subtracting the heartbeat signal from the original S_{21} phase, the phase noise is obtained. Fig. 11 presents the phase noise for different emitted powers.

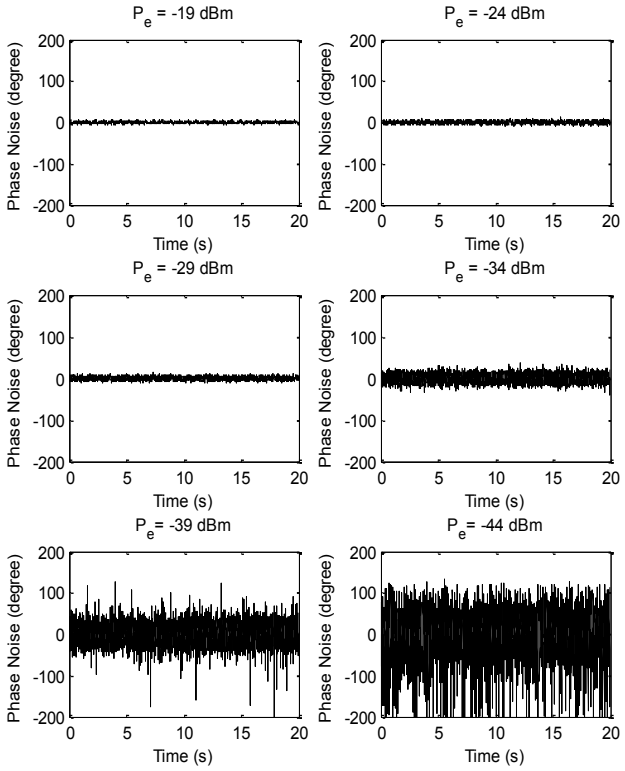

Fig. 11 Phase noise at P_e = -19, -24, -29, -34, -39 and -44 dBm and f_e = 20 GHz.

Since the noise is Gaussian, the mean value is null; hence, the variance of the phase noise (deg^2) is calculated using the following relation: The analysis of the obtained noise shows that it can be modeled as a zero mean Gaussian signal. Its variance (deg^2) can be computed using the following relation:

$$\sigma^2 = \frac{1}{N}\sum_{0}^{N-1}\left(phasenoise(i)\right)^2 \quad (13)$$

where N = 12801 is the samples number. Table 7 presents the variance of the noise for each emitted power. Fig. 12 presents the variation of phase noise variance vs. the emitted power. Finally, Fig. 13 presents the noise variance as a function of the power of the signal at the input of the VNA for a fixed person placed at 1 m from the measured system.

Table 7 Variance of the phase noise at P_e = -19, -24, -29, -34, -39 and -44 dBm and f_e = 20 GHz

Emitted Power Pe (dBm)	Variance σ^2 (deg^2)
-19	3.9
-24	7.5
-29	11.8
-34	75.7
-39	470.9
-44	1776.8

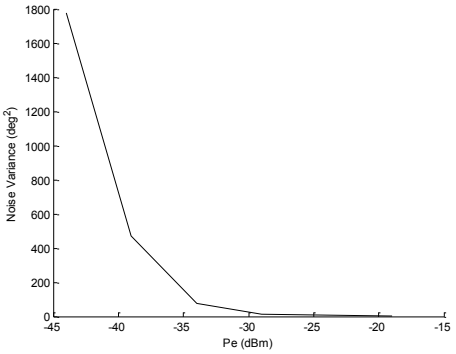

Fig. 12 Phase noise variance vs. emitted power at 20 GHz

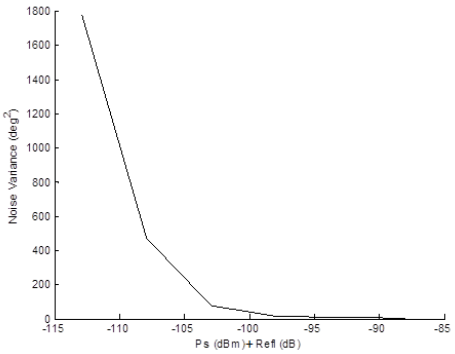

Fig. 13 Phase noise variance vs. signal power at VNA input at d = 1 m and fe = 20 GHz

On the other hand, the signal power at the VNA input is calculated in function of the distance for a certain emitted powerP_e. The person is walking for a distance between 1 and 3 m far from the system. Fig. 14 presents the signal power at VNA input subtracted by the reflection loss for a distance between 1 and 3 m at $P_e = -19dBm$.

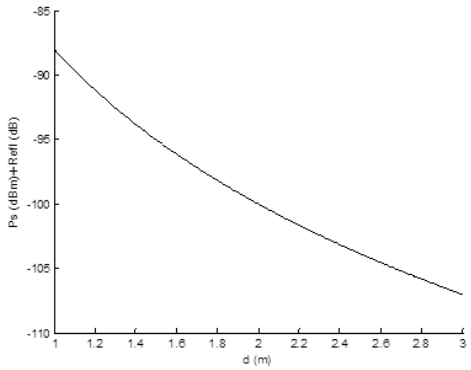

Fig. 14 Signal power at VNA input vs. distance at P_e = -19 dBm and f_e = 20 GHz,

The phase noise variance as a function of the distance is presented. Signal power at VNA input subtracted by reflection loss is between -87.88 and -112.88 dBm for a fixed person set at 1 m far from the system at emitted power varied from -19 dBm to -44 dBm. The interval of variation of signal power at VNA input subtracted by reflection loss for a distance ranging between 1 and 3 m at -19 dBm is between -87.88 dBm and -107 dBm. Fig. 15 presents phase noise model vs. time for a person moving toward the system at 20 GHz and at emitted power of -19 dBm. Starting from 3 m to 1 m, this walk takes 8 s.

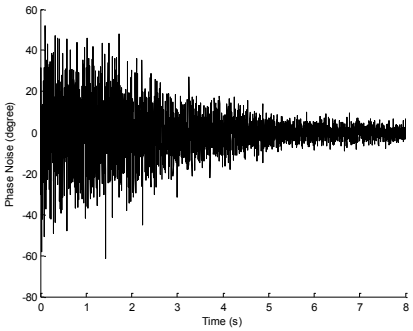

Fig. 15 Phase noise model for a person moving toward the VNA system at f_e = 20 GHz and P_e = – 19 dBm walking from d = 3 m to d = 1 m at a velocity v = 0.25 m/s

4.3 Phase variation of chest movement of a walking person at 20 GHz

Fig. 16 presents the phase variation for a person chest movement, due to his walking toward the system with a constant velocity of 0.25 m/s, starting at a distance of 3 m far from the system and stopping at a distance of 1 m, without taking into consideration the phase permutation between -180 and 180 degrees.

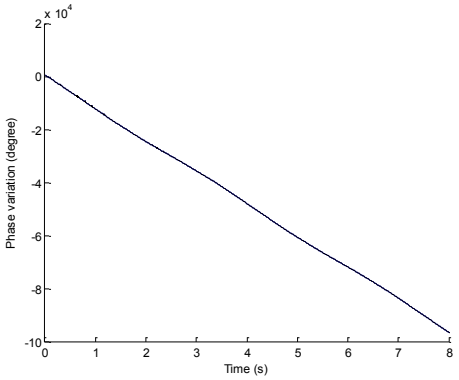

Fig. 16 Phase variation due to a person chest moving toward the VNA system at 20 GHz

Because the phase variation is between -180° and 180°, permutations from -180° to 180° and from 180° to -180° are done each time the phase variation reaches the -180° and 180° respectively. Fig. 17 and Fig. 18 present the phase variation of a walking person chest at the first 0.5 s and the last 0.5 s, respectively.

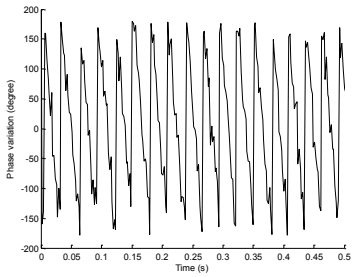

Fig. 17 Phase variation of a moving person at first 0.5 s due to respiration, heartbeat and noise at 20 GHz

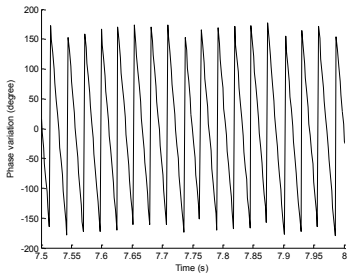

Fig. 18 Phase variation of a moving person at last 0.5 s due to respiration, heartbeat and noise at 20 GHz

Because the distance at first 0.5 s is higher than last 0.5 s, the variation of the phase at the first 0.5 s is noisier than last 0.5 s.

4.4 Signal processing and results

Before applying signal processing, all permutations between the -180° and 180° are removed, because these permutations affect the cardiopulmonary signal. Permutations elimination is done each time the phase difference between the current sample and the previous sample is equal or slightly less than 360°. Note that the respiratory and heartbeat signals are hidden because of the presence of the movement; hence, signal processing is required to extract the heartbeat signal from the phase variation. Wavelet decomposition is used as the signal processing technique for the heartbeat extraction. The sampling frequency is 512 Hz; it is chosen to avoid resampling. Hence, S_{D18} decomposition contains frequencies higher than 1 Hz. Therefore, S_{D18} contains the heartbeat frequency. Bior 2.4 is the selected wavelet for this signal because it has the smallest *RMSE* compared to the other wavelet families. Fig. 19 presents the S_{D18} applied on model for the heartbeat extraction.

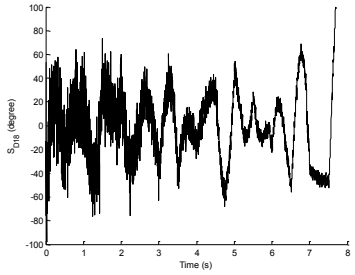

Fig. 19 S_{D18} applied on the model for heartbeat extraction at P_e = -19 dBm and f_e = 20 GHz

Because the signal is noisy, especially between t = 0 and 2 s, a sliding uniform smoothing window with n = 199 is used to eliminate the noise before applying peak detection. Fig. 20 presents the peak detection applied to S_{D18} signal and the heartbeat model.

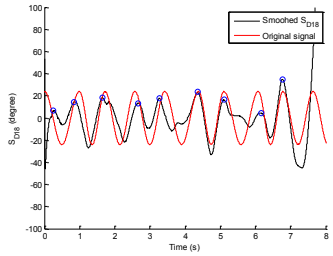

Fig. 20 Peak detection applied on S_{D18} signal and heartbeat model at P_e = -19 dBm and f_e = 20 GHz

After peak detection, the heartbeat rate extracted from S_{D18} is equal to 73.65 bpm, while the heartbeat rate of the signal model is 70.73 bpm. Hence, the relative error is equal to 4% which is acceptable. As a conclusion, wavelet decomposition is able to extract the heartbeat signal even in the presence of a walking person with a forward movement.

5 Conclusion

This work provides a comparative approach between one- and two-antennas microwave systems, and proves as well the possibility of tracking the heartbeat activity of a person while moving. When holding the breath, both, one- and two-antenna systems show an accuracy of about 93% in terms of HR. When breathing normally, using the single-antenna microwave system allows the extraction of the heartbeat rate with maximum error of 4 %. However, wavelet transform is required for processing the signals. The accuracy of the obtained results is convenient due to the relative high operating frequency, allowing quite large phase variations of the measured *S* parameters. Another scenario was performed for a person moving toward the system. This scenario is based on modeling, where parameters used in measurements are considered for modeling such as the operational frequency (20 GHz) and the transmitted power (-19 dBm). In addition, the modeling takes into consideration the noise variation according to the distance of the person from the system. Using the wavelet transform as processing tool shows the ability to extract the heartbeat rate even with presence of body movement. Future work should focus on considering different scenarios such as the presence of random body movements, obstacles, clutters, etc., and for distance greater than 3 meters.

References

1. J. C. Lin, J. Kiernicki, M. Kiernicki, and P. B. Wollschlaeger. Microwave Apexcardiography. *IEEE Trans. on Microwave Theory and Techniques*, 1979, Vol. 27, No. 6, pp. 618-620.
2. A. Rahman, E. Yavari, G. Xiaomeng, V. Lubecke, O. Boric-Lubecke. Signal processing techniques for vital sign monitoring using mobile short range Doppler radar. *IEEE conference on Biomedical Wireless Technologies, Networks, and Sensing Systems (BioWireleSS)*, pp. 1-3, San Diego, CA, 25-28 Jan., 2015.
3. Y. Wang, Y. Yang, A.E. Fathy. Reconfigurable ultra-wide band see-through-wall imaging radar system. *IEEE Antennas and Propagation Society International Symposium*, pp. 1-4, June 2009, North Charleston, SC, USA.
4. M. He, Y. Nian, Y. Gong. Novel signal processing method for vital sign monitoring using FMCW radar. *Journal in Biomedical Signal Processing and Control*, Vol. 33, pp. 335-345, March 2017.
5. L. Crocco, V. Ferrara. A review on ground penetrating radar technology for the detection of buried or trapped victims. *IEEE*

International conference on Collaboration Technologies and Systems (CTS), pp. 535–540, May 2014, Minneapolis.

6. L. Lu, C. Li, J.A. Rice. A software-defined multifunctional radar sensor for linear and reciprocal displacement measurement. In Wireless Sensors and Sensor Networks (WiSNet). *IEEE Topical Conference,* 2011, Phoenix, AZ, USA.
7. C. Gu, R. Li, C. Li, S-B. Jiang, Doppler radar respiration measurement for gated lung cancer radiotherapy. In Biomedical Wireless Technologies. *Networks, and Sensing Systems (BioWireleSS)*, pp. 91-94, January 2011, Phoenix, AZ, USA.
8. O. Boric-Lubecke, A. D. Droitcour, V. M. Lubecke, J. Lin, and G. T. A. Kovacs. Wireless IC Doppler for Sensing of Heart and Respiration Activity. *IEEE TELSIKS 2003, Serbia and Montenegro, Nis*, October 1-3 (2003), 337-344.
9. http://www.webmd.com/lung/counting-respiration-rate
10. D. Obeid, S. Sadek, G. Zaharia, G. El Zein. Noncontact heartbeat detection at 2.4, 5.8 and 60 GHz: A comparative study. *Microwave and Optical Technology Letter*, Vol. 51, No. 3, pp. 666-669, March 2009.
11. D. Obeid, G. Zaharia, S. Sadek, G. El Zein. ECG vs. single-antenna system for heartbeat activity detection. *4th International Symposium on Applied Sciences in Biomedical and Communication Technologies (ISABEL)*, October 2011, Barcelona, Spain.
12. American National Standard, Cardiac monitors, heart rate meters, and alarms, ANSI/AAMI EC1.
13. S. El-Samad, D. Obeid, G. Zaharia, S. Sadek, G. El Zein. Contact-Less measurement system or cardiopulmonary activity. *Proc. of 2014 Mediterranean Microwave Symposium (MMS)*, 2014, December 2014, Marrakech.
14. R. Motard, B.Joseph. Wavelet application in chemical engineering. *Washington University in St. Louis, springer science + business media.*
15. A. Blackburn, J. Garke Ferwerda. Retrieval of chlorophyll concentration from leaf reflectance spectra using wavelet analysis. *Remote Sensing of Environment*, Vol. 112, No. 4, pp. 1614-1632, April 2008.
16. C. Stolojescu, I. Railean, S. Moga, A. Isar. Comparison of wavelet families with application to WiMAX traffic forecasting. *International Conference on Optimization of Electrical and Electronic Equipment*, May 2010, Brasov, Romania.
17. P. Hao. Reversible resampling of integer signals. *IEEE Transactions on Signal Processing*, Vol. 57, No. 2, pp. 516-525, February 2009.
18. K.-M. Chen, Y. Huang, J. Zhang, and A. Norman. Microwave life-detection systems for searching human subjects under earthquake rubble or behind barrier. *IEEE Transaction in Biomedical Engineering*, Vol. 27, No. 1, pp. 105–114, January 2000.
19. D. T. Petkie, C. Benton, E. Bryan. Millimeter wave radar for remote measurement of vital signs. *IEEE Radar Conference*, pp. 1-3, 2009.
20. I. Nasr, E. Karagozler, I. Poupyrev, S. Trotta. A highly integrated 60-GHz 6-Channel transceiver chip in 0.35 µm SiGe technology for smart sensing and short-range communications. *IEEE Compound Semiconductor Integrated Circuit Symposium (CSICS)*, pp. 1-4, October 2015, New Orleans, LA, USA.
21. J. Tu, T. Hwang, Member, J. Lin, Fellow. Respiration rate measurement under 1-D body motion using single continuous-wave Doppler radar vital sign detection system. *IEEE Transactions on Microwave Theory and Techniques*, Vol. 64, No. 6, pp. 1937-1946, June 2016.
22. P. Singh, V. K. Babbar, A. Razdan, T. C. Goel, S. L. Srivastava. Magnetic, dielectric and microwave absorption studies of Ba-CoTi haxaferrite-epoxy composites. *Indian Journal of Pure and Applied Physics,* Vol. 42, pp. 221-228, March 2004.

AUTHORS' INFORMATION

Sarah Samad was born in Senlis, France in 1988. She received Diploma in electrical and electronics engineering from Lebanese University, Tripoli, Lebanon and Master Degree in technologies of medical and industrial systems. She got her Ph.D. degree at INSA of Rennes, France and the Lebanese University, Lebanon. Her research interests are on cardiopulmonary detection using Doppler radar.

Gheorghe Zaharia received the B.S. degree in electronics and telecommunications from the Polytechnic Institute of Iasi, Romania, in 1981 and the D.E.A. and Ph.D. degrees in telecommunications, signal processing and electronics from the "Institut National des Sciences Appliquées » (INSA) of Rennes, France, in 1991 and 1997, respectively.
From 1983 to 1990 he was a Lecturer at the Technical University of Iasi, Romania. Between 1983 and 1985 he studied mathematics at the University "Al. I. Cuza" of Iasi. Since 1997, he is Associate Professor in the Department "Communications Systems and Networks", the former "Electronics and Communications Systems" Department, INSA, Rennes. His teaching and research interests mainly concern the study of radio waves propagation, communications systems, information theory, and coding. Gheorghe Zaharia is Senior Member IEEE and member of the Romanian Society of Medical Bioengineering. He was member of the Scientific Committee of several international conferences (EHB 2011, EHB 2013, MMS 2013 …). He has more than 30 journal papers, about 100 papers presented at international conferences and 2 patents. He is also co-author of one book and 5 book chapters.

Sawsan Sadek received the B.S. degree in physics from Lebanese University in 1989 and Ph.D. degree in Microwaves from the University of Sciences and Technologies of Lille, France, in 1996.
Actually, Sawsan is a professor at the Lebanese University, University Institute of Technology in Saida, Lebanon, Department of Communications, Computer and Networks.

She chaired the department for 5 years from 2009 to 2014. She organized the MMS2013 in Saida, Lebanon. She participated to several scientific committees for international conferences and has more than 7 journal papers, 20 international conferences and one book chapter.

Ghais El Zein received the M.S. degree in Electronics, the Ph.D. degree in Telecommunications and Signal Processing, and the H.D.R. “Habilitation à Diriger des Recherches” degree in Electronics from the University of Rennes 1 - France, in 1983, 1988 and 1998, respectively. From 1985 to 1987, he was a Lecturer, and from 1990 to 1999, an Associate Professor, in the Department of Electronics and Communications Systems Engineering, of the “Institut National des Sciences Appliquées de Rennes” (INSA) - France, where he is currently a Professor.

He has authored or co-authored over 215 technical papers in major international journals and conferences, 2 books, 13 book chapters and 4 patents in the areas of communications and radio propagation. His teaching and research interests mainly concern the study of radio wave propagation phenomena and the evaluation of their effects on communication systems.

Prof. El Zein served as a TPC member and symposium chair of several international conferences. From 2001 to 2009, he served as deputy director of the Institute of Electronics and Telecommunications of Rennes (IETR - UMR CNRS 6164). Since 2009, he is the Head of Radio Propagation Team. He is a member of URSI-F and member of the Monitoring and Assessment Committee (CSE) of the “Images et Réseaux” cluster.

Dany Obeid has received his BS degree in Computer Engineering from University of Balamand, an M.S degree in Computer and Communications Engineering from the American University of Science and Technology, and a PhD degree in Telecommunications and Signal Processing from INSA of Rennes, in 2003, 2006, and 2010 respectively. Dany worked as a lecturer and researcher in INSA of Rennes and the Lebanese University, and as an R&D engineer in Kaptalia Monitoring.